

# EECS C145B / BioE C165: Image Processing and Reconstruction Tomography

## Lecture 16

Jonathan S. Maltz

**This handout contains copyrighted material. It is for personal educational use only. Do not distribute.**

jon@eecs.berkeley.edu  
<http://muti.lbl.gov/145b>  
510-486-6744

1

## Topics covered

1. History of ultrasonic imaging
2. The A-mode scan
3. The piezoelectric transducer
4. The M-mode scan
5. The B-mode scan
6. Ultrasound systems
7. Multielement transducers
8. Imaging flow
9. Continuous wave Doppler
10. The sonogram
11. Pulsed wave systems
12. Ultrasound physics
13. Ultrasound computed tomography

2

## Reading

Additional reading:

- Cho, “Foundations of Medical Imaging”, John Wiley and Sons (1993), Chapters 14 and 15.
- Webb, “The Physics of Medical Imaging”, Institute of Physics Publishing (1998), Chapter 7.
- Jensen, “Estimation of Blood Flow Velocities Using Ultrasound”, Cambridge University Press (1996), Chapters 1 and 2.
- Kak and Slaney, “Principals of Computerized Tomographic Imaging”, IEEE Press (1998), pp. 147-158. Available free at: <http://rvl4.ecn.purdue.edu/~malcolm/pct/>

3

## History of ultrasonic imaging

- Medical ultrasound imaging dates back to the 1950s. Wild (1950), and Howard and Bliss (1952) in the USA, and Edler and Hertz (1954) in Europe, demonstrated that ultrasound could be used for:
  1. Detecting tissue layers
  2. Identifying tumors
  3. Imaging structures in the heart
- Ultrasonic waves are generated using **piezoelectric transducers**.
- These waves **propagate** through tissues and are **reflected, scattered and attenuated**.
- The **backscatter signal** is usually received at the same transducer that **insonated** the tissue.

4

## History of ultrasonic imaging

- A **time gain compensation (TGC) amplifier** is used that amplifies the signal more as time elapses so that signals returned from a greater depth are amplified to **compensate for the greater attenuation experienced by these waves**.
- The **dynamic range** of the returning signal is so **large** that it must be **compressed in amplitude** (using logarithmic compression, for example) for display purposes.
- The first scanners displayed the envelope of the ultrasound carrier frequency. **This time domain signal shows the intensity of backscatter as a function of depth.**
- Assuming the speed of sound is constant in tissue (1540 m/s, a good assumption in soft tissues), **depth is linearly proportional to time.**
- The graph of this time domain signal is called the **A-line**. The first scanners operated in **A-mode**. “A” stands for “amplitude”.

5

## History of ultrasonic imaging: the first scanners

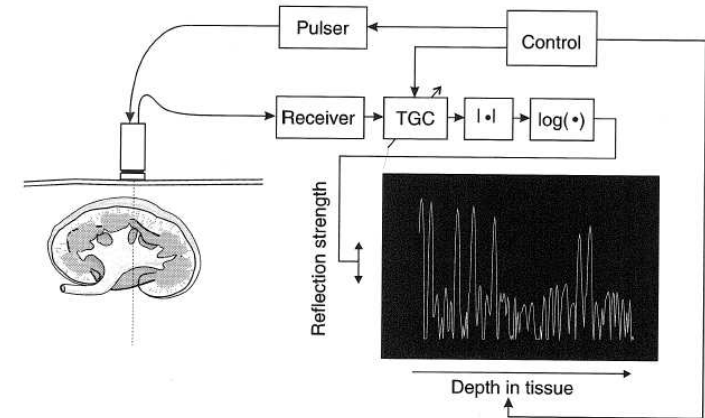


Fig. 1.1. Simple A-mode system.

Source: Jensen p. 2

The independent variable in the graph of the A-line is **arrival time**. Depth is linearly proportional to the time of the arrival of the backscatter.

6

## The piezoelectric transducer

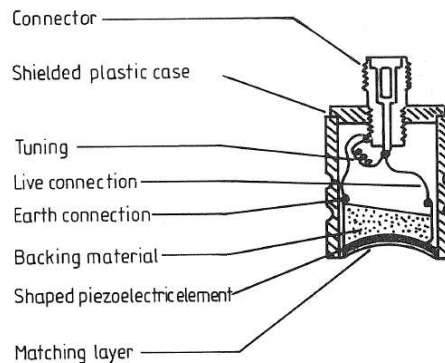


**Figure 7.10** Typical components in the design of a conventional single-element ultrasonic transducer.

Source: Webb p. 338

Piezoelectric materials expand or contract along an axis depending on the applied voltage. When operated at sonic and ultrasonic frequencies, pressure waves are produced. When returning pressure waves interact with piezoelectric material, a voltage is produced. The transducer acts as a loudspeaker as well as a microphone.

7

## The M-mode scan

- An A-mode scan does **not provide much structural information**. It is useful primarily for **determining motion**, such as that of the heart.
- In an **M-mode scan**, several A-mode lines, successively acquired in time, are placed side-by-side and displayed as an image.
- The image **graylevel is proportional to the amplitude of the A-line**. Its **horizontal axis is time**. Its **vertical axis is depth**.
- The M-mode image is a horizontal scrolling **movie** showing how the distribution of backscatterers along a **single line** changes with time. “M” stands for “motion”.
- M-mode is very useful for monitoring temporal changes in the diameter of arteries. These scans can also be used to determine the elasticity (distensibility) of vessels.

8

## Scanning in M-mode

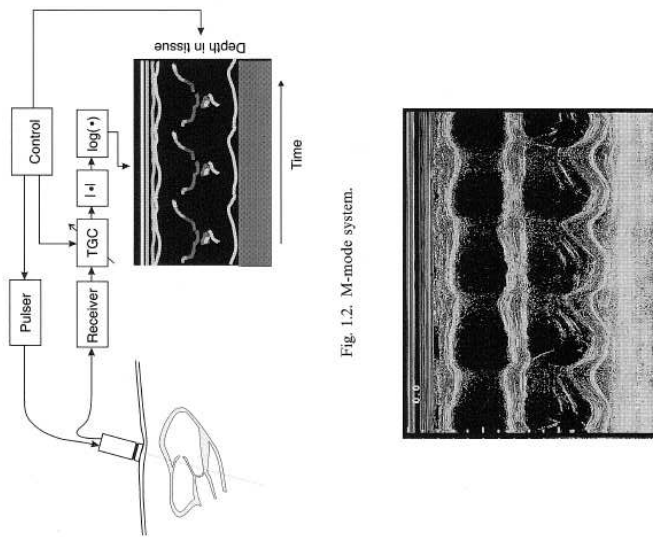


Fig. 1.2. M-mode system.

Source: Jensen p. 3

## The B-mode scan

- A- and M-mode scans interrogate only a **single spatial dimension**. 2D imaging is accomplished using **B-mode imaging**. “B” stands for “brightness”.
- B-mode imaging is accomplished by **combining many A-lines acquired along different directions into a single 2D image**.
- The first scanners used a **mechanical arm** with position encoding to sample all of the A-lines. Owing to the low speed of operation, real-time imaging was not possible.
- The next generation of scanner used a **servo motor** to sweep a single piezoelectric crystal through an arc in order to sample a 2D slice.
- Advances in electronics allowed **multielement transducers** to be employed. **Electronic steering and focusing** of the beam became possible. Modern 2D ultrasound scanners have **no moving parts**.

## Scanning in B-mode: mechanical arm scanning

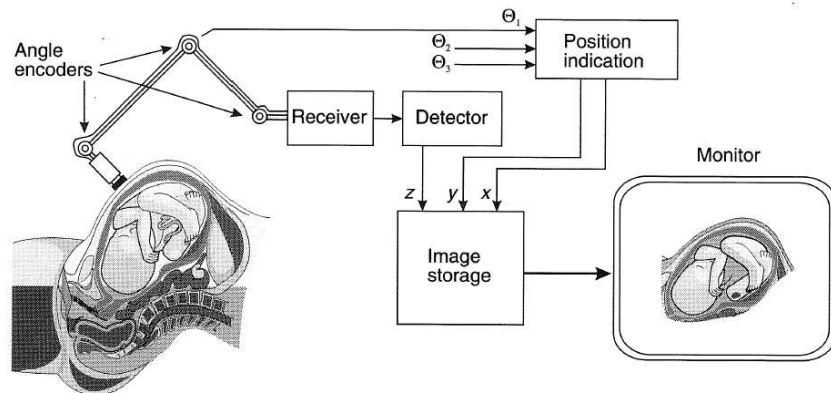
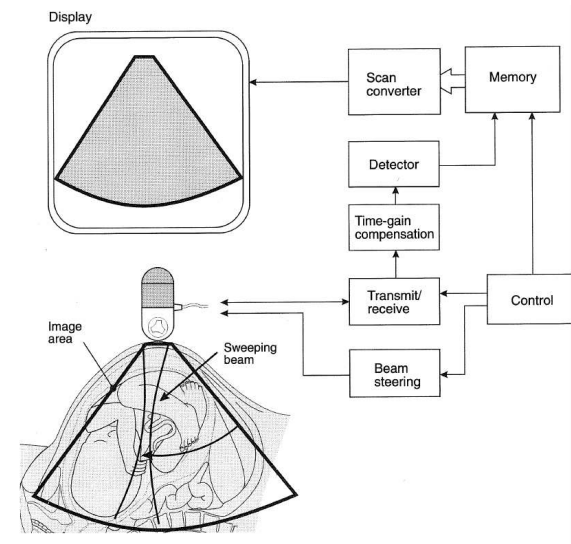


Fig. 1.4. System for acquiring static B-mode images.

Source: Jensen p. 4

## Scanning in B-mode: real-time electronic scanning



Source: Jensen p. 5

## Ultrasound systems: contemporary multielement systems



Source: Siemens Medical (right)



13

## Ultrasound systems: block diagram

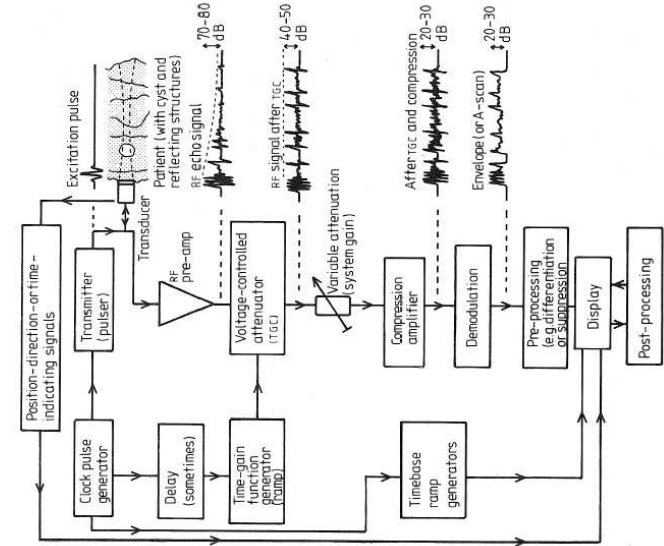


Figure 7.13 Block diagram of the essential components in the signal-processing chain of an ultrasound pulse-echo imaging system. On the right of the figure are labelled schematic versions of the kind of signal one might expect to observe at the points indicated, in response to a single transmitted sound pulse.

Source: Webb p. 344

14

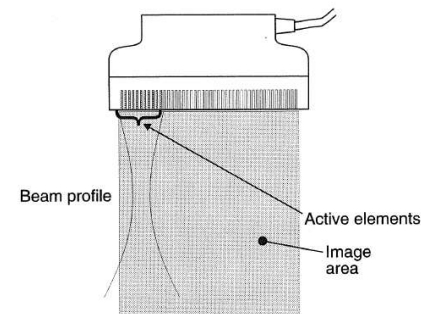
## Multielement transducers

- There are two types of modern transducer. These are classified according to the method by which they direct the beam.
- **Linear transducers** activate elements **directly over the region being imaged**. The beam is thus **not steered electronically**. It can be **focused to a certain depth in receive mode**.
- Typical linear transducers consist of 256 elements. Thus, 256 A-lines can be scanned at a **single transducer position**. Signals to and from the elements are **delayed** so as to approximate a concave wavefront.
- **Phased array transducers steer the beam electronically**. The ultrasound carrier applied to each crystal is phase shifted to effect steering. **All of the elements are used simultaneously**.
- Linear transducers produce a rectangular scan.
- Phased array transducers produce a sector scan.

15

## Scanning in B-mode: real-time electronic scanning

### Linear array transducer



### Phased array transducer

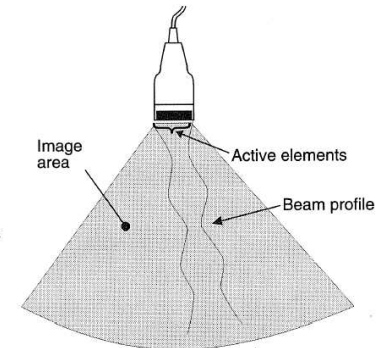


Fig. 1.6. Linear and phased array transducers. The linear array is shown with a fixed focus in both transmit and receive. The idealized beam pattern for the phased array is for one transmit focus and three different receive foci.

Source: Jensen p. 5

16

## Probes for B- and M-mode

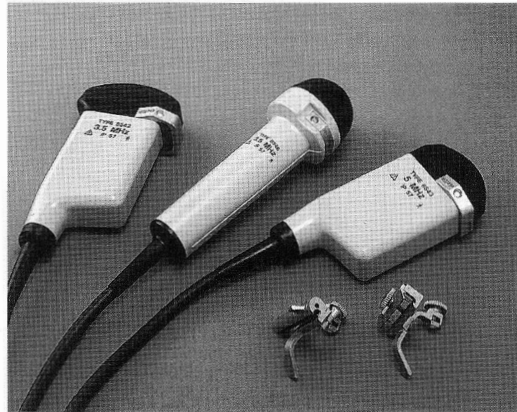


Fig. 1.7. Commercially obtainable ultrasound transducers. The transducers are from left to right: 3.5 MHz convex, linear array, 3.5 MHz annular array, and 5 MHz convex array. All three are used for obtaining real-time B-mode images primarily from the abdomen. The fixtures shown are guides for biopsy needles (photo courtesy of B&K Medical A/S, Denmark).

Source: Jensen p. 6

17

## Probes for B- and M-mode

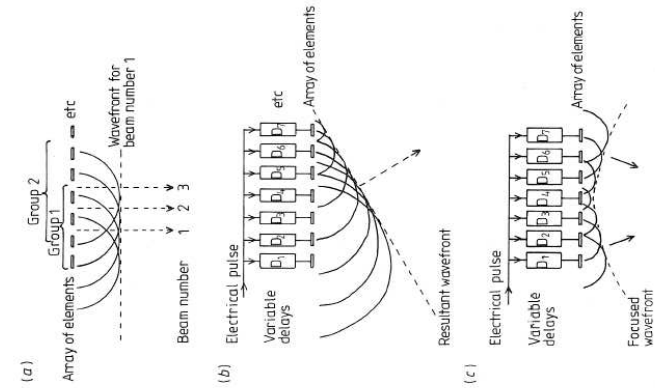


Figure 7.11 Schematic, two-dimensional illustration of the principles of beam forming ((a), (b) and (c)), focusing (c), lateral scanning (a) and steering (b), using arrays of elemental sound sources.

Source: Webb p. 341

18

## Probes for B- and M-mode

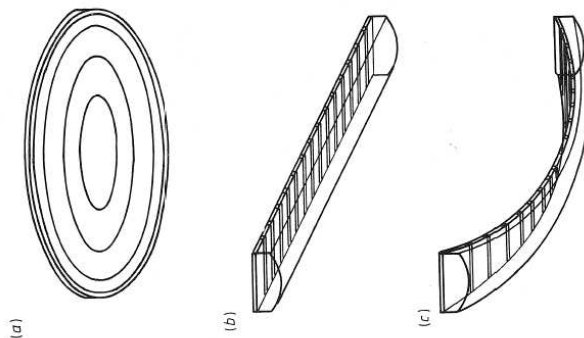


Figure 7.12 Two main transducer array configurations currently in use: (a) annular array (often prefocused by shaped ceramic or a lens, so that the maximum electronic delay between elements is minimised) and (b) linear array (shown with a fixed focus in the plane orthogonal to the scan plane). (c) The linear array is sometimes laid down on a curved surface to produce a sector-type image without phase-controlled beam steering.

Source: Webb p. 342

19

## Probes for B- and M-mode

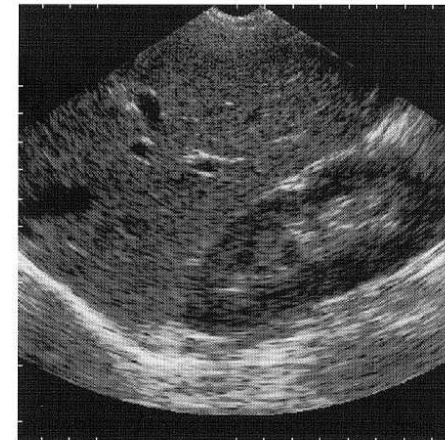


Fig. 1.8. Image acquired by a B-mode system of liver and the right kidney of a healthy, 27 year old male. The image was acquired by a 3.5 MHz transducer with a concave, rotating crystal. The markers at the side of the image indicate 1 cm.

Source: Jensen p. 7

20

## Probes for B- and M-mode

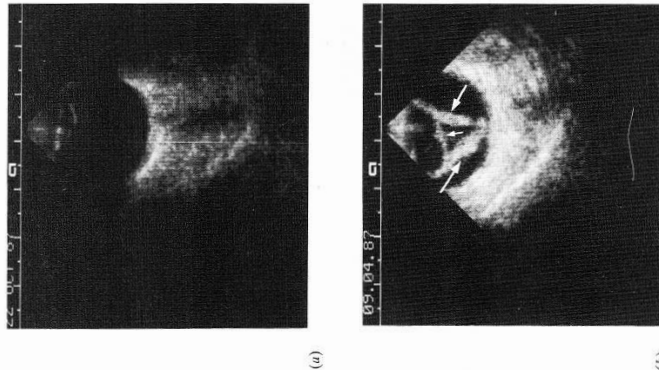


Figure 7.26 Sector B-scan of the normal eye (a) and another depicting multiple retinal detachments (b). (Courtesy of M Restori.)

Source: Webb p. 374

Phased array probes are especially useful for examining spherical objects such as the eye ball.

21

## Probes for B- and M-mode

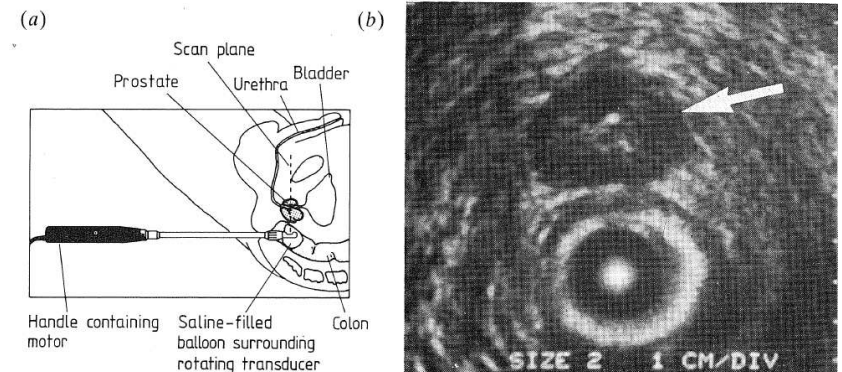


Figure 7.21 Diagram of assembly and mechanics of one type of transrectal ultrasound probe (a) and a typical image, showing cancer of the prostate (indicated by white arrow), obtained with this system (b). (Diagram adapted from sales brochure of Bruel and Kerr Ltd; grey scale image courtesy of D O Cosgrove.)

Source: Webb p. 360

22

## Imaging flow

- Blood scatters ultrasound.
- When a blood vessel is insonated with a continuous ultrasound carrier of frequency  $f_0$ , the backscattered signal will have a frequency component:

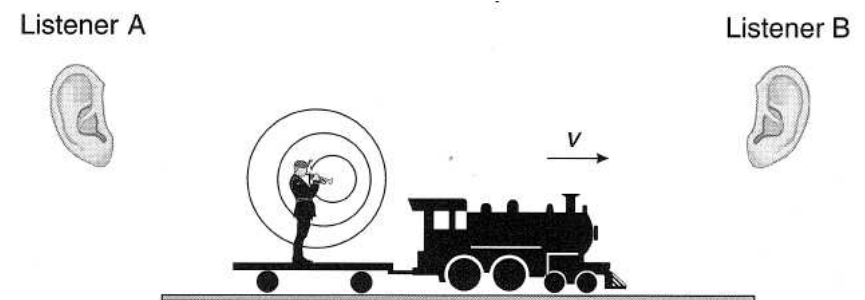
$$f' = f_0 \frac{c + v_o}{c + v_s}$$

where  $v_s$  is the speed of a red blood cell scatterer,  $v_o$  is the speed of the observer (usually zero in ultrasonic imaging), and  $c$  is the speed of sound in tissue.

- **The observed shift in the carrier frequency is thus a measure of blood flow.**
- Satomura (1957) was the first to implement this application of **continuous wave (CW)** ultrasound for blood flow measurement.
- CW is useful for detecting vessel occlusion, reactive hyperemic flow, the pulse flow waveform, heartrate and fetal heart beat. Most Doppler stethoscopes employ CW Doppler.

23

## CW Doppler flow measurement



Source: Jensen p. 8

Due to wavefront compression, the sound heard by listener B has higher pitch than the sound heard by the trumpet player. Listener A hears a lower pitch than the other observers. In CW ultrasound, the train is replaced by a red blood cell and the trumpetter by backscattered insonation. What is inaccurate about this analogy?

24

### CW Doppler flow measurement

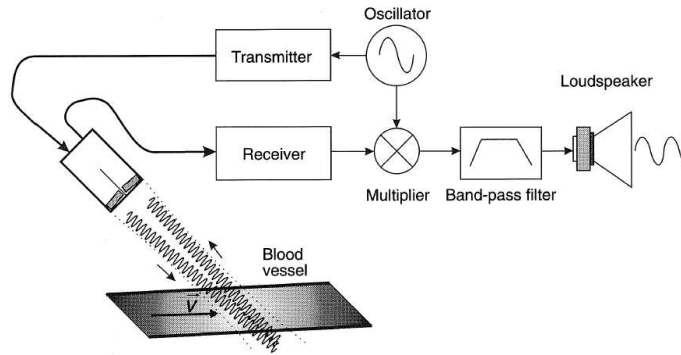


Fig. 1.10. Continuous wave Doppler system.

Source: Jensen p. 8

The transmitter applies a ultrasound carrier in the range of 1 – 15MHz. The speed of moving red blood cells is such that the **Doppler shift** is usually between DC and several kHz. This is **in the human auditory range**. Multiplying the transmitted and received signals produces a **beat frequency** that is equal to  $|f' - f|$ .

25

### CW Doppler flow measurement

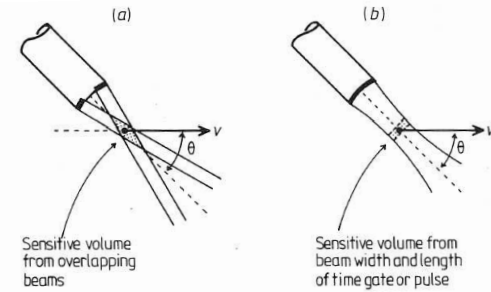


Figure 7.5 Two types of Doppler system, the continuous wave (a) and the pulsed wave (b) illustrating the angle  $\theta$ , which is of significance in the backscatter Doppler equation (7.10).

Source: Webb p. 327

For oblique insonation, the CW system to the left records a Doppler shift:

$$\Delta f = f - f_0 = \frac{\pm 2f_0 v \cos \theta}{c}$$

where  $v$  is the mean velocity of the insonated volume. This shift is double that observed by a stationary observer and moving source. Why?

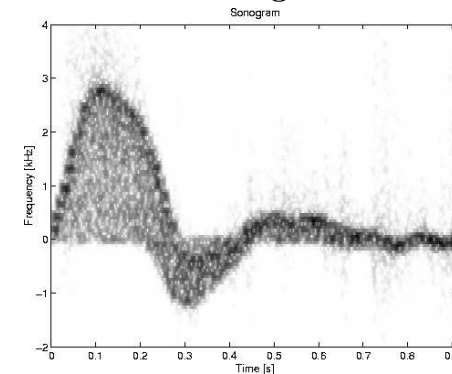
26

### The sonogram

- In CW Doppler, **each insonated red blood cell** produces some backscatter.
- The signal received therefore contains the contributions from **thousands of cells**, each moving at a **different speed**.
- **Fourier analysis** can be used to determine how many cells are moving within a range of speeds.
- The discrete Fourier **power spectrum** of the CW system output is therefore a **histogram of red blood cell velocities**.
- This output is conventionally displayed as a **sonogram**.
- The sonogram shows the time evolution of the spectrum.
- The sonogram is an **image whose horizontal axis is time**.
- The **vertical axis is frequency shift (or velocity)**.
- The **brightness of each point** is proportional to the **number of cells traveling at a specific speed**.

27

### The sonogram



Source: Jensen website

This sonogram shows blood flow in the femoral artery during a single cardiac cycle. Here, the **darker a pixel**, the **more cells** are reflecting that specific frequency, and so are traveling the corresponding velocity. We see that most of the cells are traveling at the maximum velocity during the systolic segment. This is typical of non-laminar “plug” flow.

28

## The sonogram

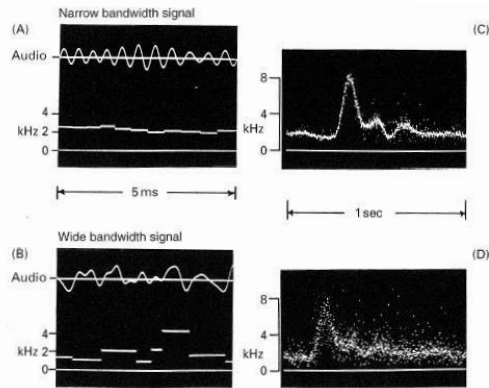


**Fig. 7.8** Illustration showing the effect of sample volume dimensions or the width of the Doppler spectrum as measured by the zero-crossing interval histogram (ZCIH) method. The upper signals (A, C) were made using a 20 MHz pulsed Doppler with a single-range gate centered in the radial artery. The lower signals (B, D) were made by summing the audio signals from eight gates spaced across the radial artery from near to far walls. The velocity gradient in the single sample volume is small, the interval between zero-crossings of the audio signal is uniform (A) and the resulting spectrum is narrow (C). The velocity gradient across the entire vessel is large, the interval between zero-crossings of the audio signal is variable (B) and the resulting spectrum is wide (D). The width of the spectrum is a measure of the velocity gradient in the sample volume. In this case, the spectrum is wide because the sample volume is large relative to the vessel. A wide spectrum with a small sample volume is usually related to flow disturbances (see Fig. 7.13)

Source: Macdonald p. 162

29

## Constructing a sonogram

Given: Audio output of Doppler system

1. Sample the output using an A/D converter.
2. Select a time-window of 5 to 20 ms of samples.
3. Apply the FFT to these samples.
4. Find the square of the magnitude of the FFT.
5. Take the first half of this vector (positive frequencies) and place this column vector in a matrix so that the DC component is located at the bottom left of the matrix.
6. Select the next 5 to 20 ms of signal and repeat, placing the power spectrum column vector at column 2 of the matrix.
7. Repeat until all columns are filled.
8. Display matrix as a graylevel image.

Most ultrasonic imagers display the sonogram in real time horizontal scroll mode.

31

## The sonogram

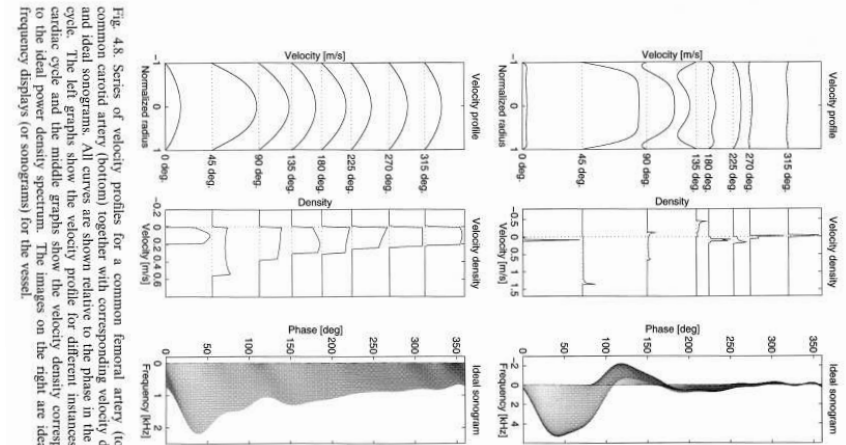


**Fig. 4.8** Series of velocity profiles for a common femoral artery (top) and common carotid artery (bottom) together with corresponding velocity densities and ideal sonograms. All curves are shown relative to the phase in the cardiac cycle. The left graphs show the velocity profile for different instances in the cardiac cycle and the middle graphs show the velocity density corresponding to the ideal power density spectrum. The images on the right are ideal time-frequency displays (or sonograms) for the vessel.

Source: Jensen p. 100

30

## Flow measurement: pulsed wave (PW) systems

- In CW systems, the returned signals originate from the **entire insonated volume**.
- It is **not possible to detect the depth** of a vessel using a single transducer.
- **Pulsed wave systems** apply multiple pulses of ultrasound.
- The time between the transmission of the pulse and the reception of its backscatter is recorded. **This delay is linearly proportional to blood velocity.**
- Do PW systems rely on the Doppler effect?

---

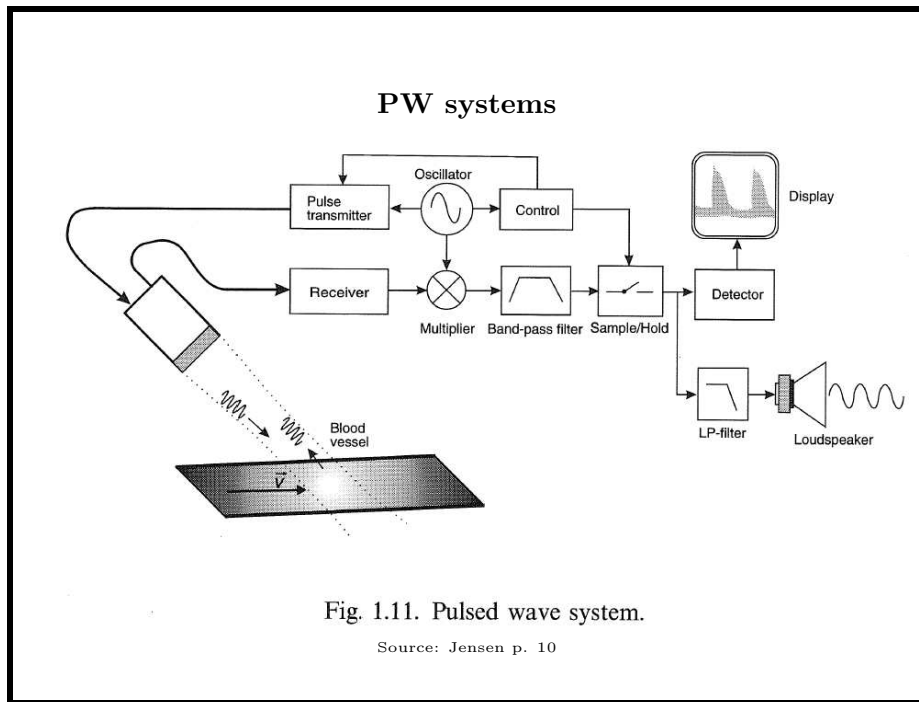


---

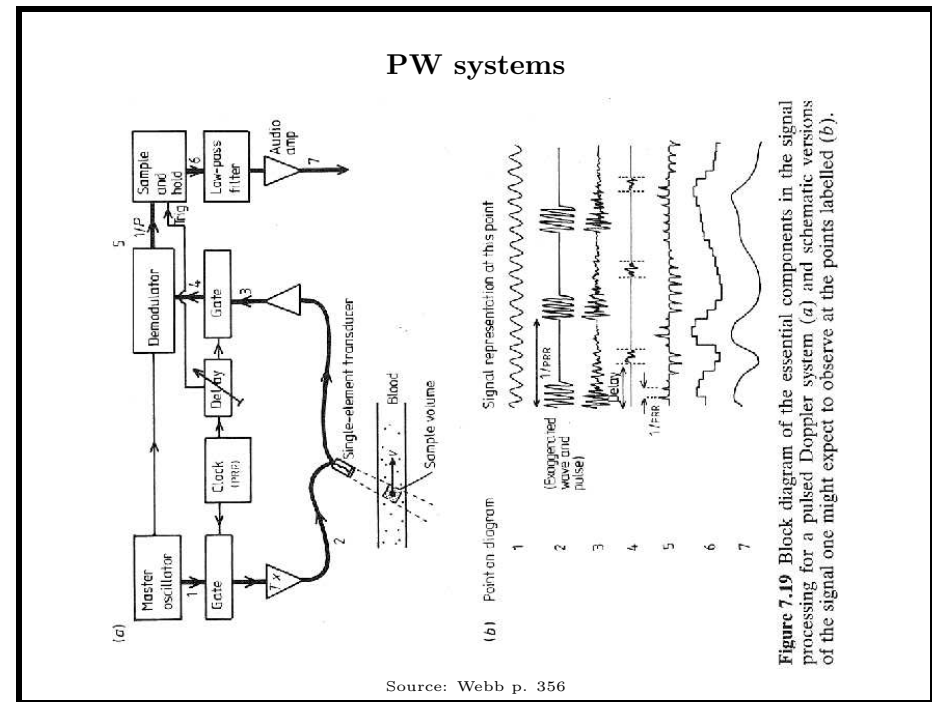


---

32



33

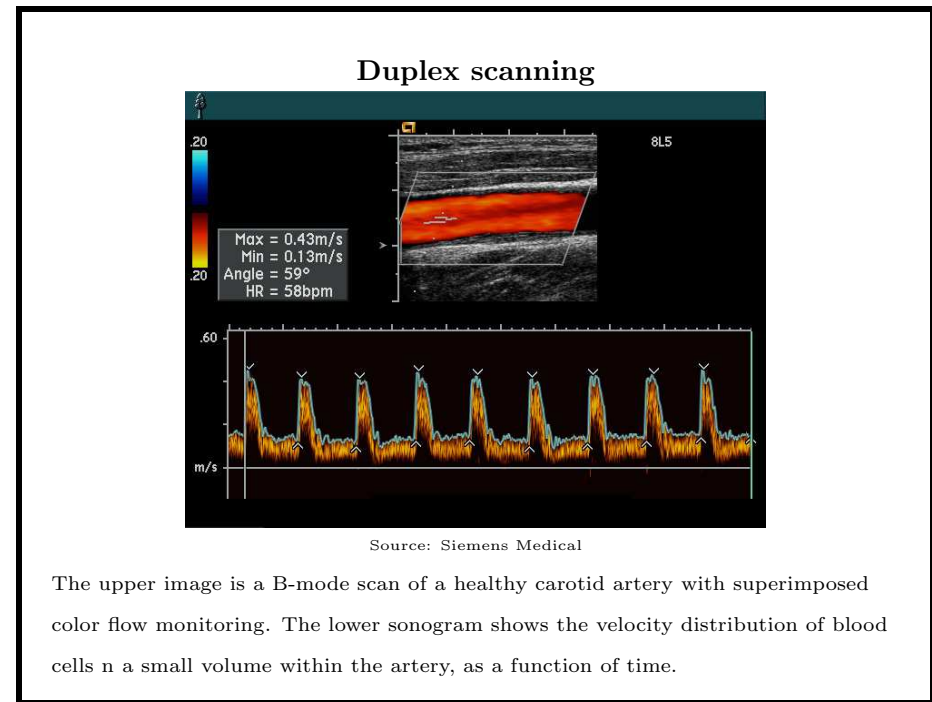


34

### Flow measurement: pulsed wave (PW) systems

- **Duplex scanners** can display B-mode images with PW velocity estimates superimposed.
- In **power/energy** mode, the **total flow power over all frequencies** is superimposed on the image.
- In **color flow** mode, pseudocolor is used to indicate both flow power and direction.
- PW allows a sonogram to be generated for flow at **any point** in a B-mode image. **Range gating** is used to extract the scatter contribution from a small volume.

35



36

## Triplex scanning

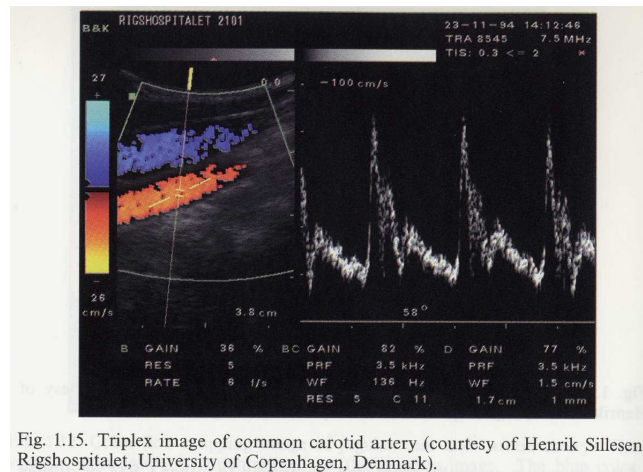


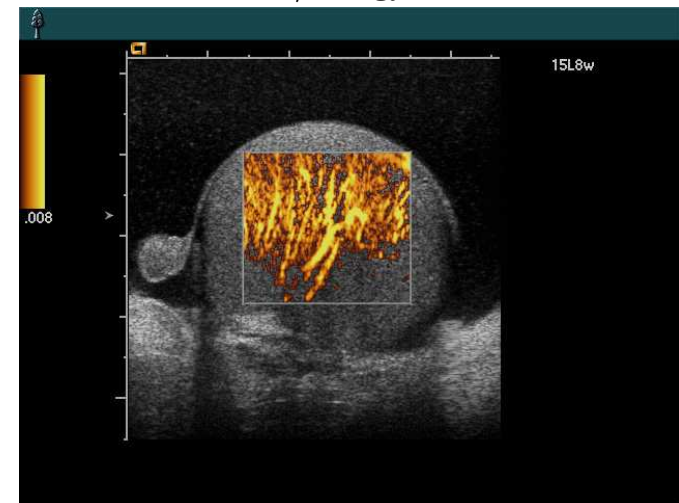
Fig. 1.15. Triplex image of common carotid artery (courtesy of Henrik Sillesen, Rigshospitalet, University of Copenhagen, Denmark).

Source: Jensen p. 14

This image shows the jugular vein above the carotid artery in B-mode with superimposed color flow information. The jugular flow is colored blue (for reverse flow) and the carotid, red, for flow away from the heart.

37

## Power/energy mode



Source: Siemens Medical

This B-mode scan with flow power superimposed shows normal testicular flow.

38

## Ultrasound physics

- Sound waves in tissues are **pressure waves** that **disturb the position of particles without any mass transport**.
- Particles **oscillate about their mean positions** in a direction **parallel** to the wave propagation direction. Such disturbances are termed **longitudinal waves**.

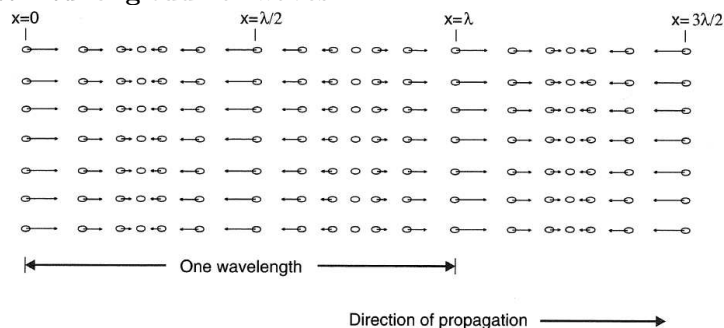


Fig. 2.1. Particle displacement for a propagating ultrasound wave at one time

Source: Jensen p. 17

39

## Ultrasound physics

- The **propagation speed** of this disturbance is given by:

$$c = \sqrt{\frac{1}{\rho_0 \kappa}}$$

where  $\rho_0$  is the mean density and  $\kappa$  is the adiabatic compressibility (assumes no heat transfer to medium).

- In water  $\kappa \approx 457 \times 10^{-12} \text{ m}^2/\text{N}$  and so  $c \approx 1480 \text{ m/s}$ .
- This assumes the **wave pressure is small compared to the equilibrium pressure**, leading to **linear propagation**.
- This assumption is **good in attenuating tissues**, but not in poorly attenuating bulk liquids such as aminotic fluid. Fetal scans consequently suffer from **non-linear artifacts** that are due to incorrect calculation of scatterer depths.

40

## Ultrasound physics: reflection and transmission

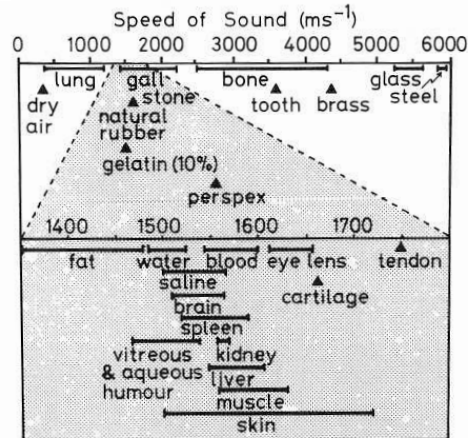


**Figure 7.1** Ranges of measured values for speed of sound in various biological and non-biological media. The data for soft tissues and biological liquids, which fall within a narrow range, are shown using an expanded scale in the shaded portion of the figure. (After Bamber (1986b), which also contains the references to the original sources of data and methods of measurement.)

Source: Webb p. 321

41

## Ultrasound physics

- The **acoustic pressure** of an harmonic **plane sound wave** of amplitude  $p_0$  propagating in the  $z$ -direction is given by:

$$p(t, z) = p_0 e^{-j(\omega t - kz)}$$

where  $\omega$  is the frequency of the wave and  $k = \frac{2\pi}{\lambda}$  is the wave number.

- The plane wave is only an approximate model for a true ultrasound field, since it assumes that the wave pressure is **independent of location in the transverse plane**.
- The spherical wave model is more important in modeling ultrasound fields:

$$p(t, r) = p_0(r) e^{-j(\omega t - kr)}$$

Because the energy in the outgoing wave must be constant, we must have  $p_0(r) = K_p/r$ , where  $K_p$  is some constant.

42

## Ultrasound physics

- The **speed of the particles** through which the wave travels is related to the wave pressure according to:

$$u = \frac{p}{Z}$$

where  $Z$  is the **characteristic impedance**.

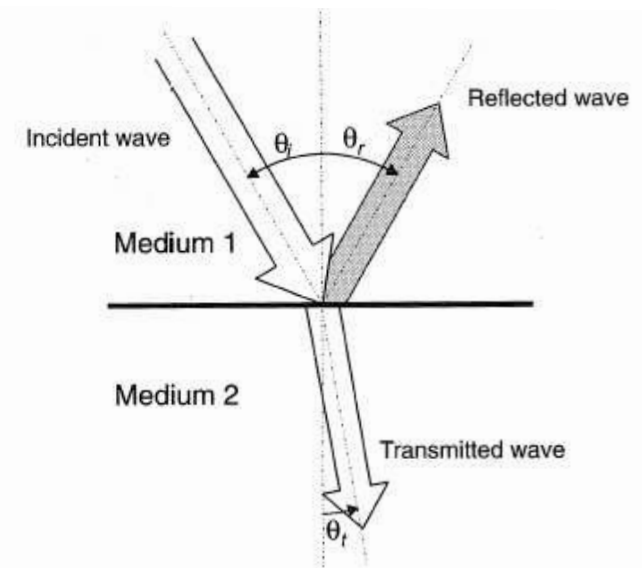
- For the plane wave:

$$Z = \rho_0 c$$

- Differences in characteristic impedance are a **fundamental source of contrast** in ultrasound images.
- This is because a wave, when encountering an interface between two media having different mean acoustic properties will be **partially transmitted and partially reflected**.

43

## Ultrasound physics: reflection and transmission



Source: Jensen p. 24

44

## Ultrasound physics: reflection and transmission

- For a wave incident normal to an interface, the pressure reflection coefficient is:

$$R_a = \frac{Z_2 - Z_1}{Z_1 + Z_2} = \frac{1 - \frac{Z_1}{Z_2}}{1 + \frac{Z_1}{Z_2}}$$

where  $Z_1$  and  $Z_2$  are the acoustic impedances of the first and second media, respectively.

- The reflection coefficient is the **ratio of the power reflected  $p_r$  to the power incident  $p_i$** .
- More generally, for oblique incidence:

$$R_a = \frac{Z_2 \cos \theta_i - Z_1 \cos \theta_t}{Z_2 \cos \theta_i + Z_1 \cos \theta_t} = \frac{p_r}{p_i}$$

where  $\theta_i$  is the angle of incidence and  $\theta_t$  is the angle of the transmitted wave.

45

## Ultrasound physics: reflection and transmission

- These angles are related by Snell's law:

$$\frac{c_1}{c_2} = \frac{\sin \theta_t}{\sin \theta_i}$$

- The **reflected wave** returns at an angle of reflection  $\theta_r = \theta_i$  with respect to the normal.
- The **transmitted wave** propagates into the second medium. The amplitude of this wave can be calculated using the **pressure amplitude transmission coefficient**:

$$T_a = \frac{2Z_2 \cos \theta_i}{Z_2 \cos \theta_i + Z_1 \cos \theta_t} = \frac{p_t}{p_i}$$

- $R_a$  from fat to air is  $-99.94\%$  (nearly all energy is reflected).
- $R_a$  from muscle to bone is  $49.25\%$  (poor return signal makes imaging difficult).
- Ultrasound is mostly useful for **soft tissue imaging** where  $|R_a| < 0.1$ .

46

## Ultrasound physics: reflection and transmission

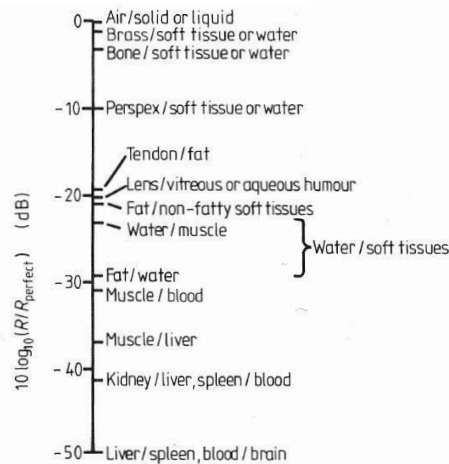


**Figure 7.4** Calculated reflection coefficients (in decibels relative to a perfect reflector) for sound at normal incidence to a variety of hypothetical boundaries between biological and non-biological media.

Source: Webb p. 326

47

## Ultrasound physics: reflection and transmission

Table 2.1. Approximate densities, sound speeds, and characteristic acoustic impedances of human tissues (data from the compilation by Goss et al. (1978) and (1980)). The speed of sound has been calculated from the density and characteristic acoustic impedance data

Medium	Density kg/m <sup>3</sup>	Speed of sound m/s	Characteristic acoustic impedance kg/[m <sup>2</sup> .s]
Air	1.2	333	$0.4 \times 10^3$
Blood	$1.06 \times 10^3$	1566	$1.66 \times 10^6$
Bone	$1.38 - 1.81 \times 10^3$	2070 - 5350	$3.75 - 7.38 \times 10^6$
Brain	$1.03 \times 10^3$	1505 - 1612	$1.55 - 1.66 \times 10^6$
Fat	$0.92 \times 10^3$	1446	$1.33 \times 10^6$
Kidney	$1.04 \times 10^3$	1567	$1.62 \times 10^6$
Lung	$0.40 \times 10^3$	650	$0.26 \times 10^6$
Liver	$1.06 \times 10^3$	1566	$1.66 \times 10^6$
Muscle	$1.07 \times 10^3$	1542 - 1626	$1.65 - 1.74 \times 10^6$
Spleen	$1.06 \times 10^3$	1566	$1.66 \times 10^6$
Distilled water	$1.00 \times 10^3$	1480	$1.48 \times 10^6$

Source: Jensen p. 19

48

### Ultrasound physics: scattering

- Thus far, we have made certain assumptions:
  1. The waves are **plane waves** (too simplistic)
  2. **Well-defined boundaries** between regions of different mean acoustic properties exist (such boundaries are rarely found in the human body and seldom show up in ultrasound images because the **reflected wave often does not reflect in the direction of the transducer**).
- Most detail in ultrasound images is due to scatter, which occurs because of **small local changes in density, compressibility and absorbtion**.
- Reflections from boundaries **far exceed scatter in magnitude**.
- Commercial scanners are **optimized to detect backscatter**. Reflections (for example those occurring at the walls of arteries) appear as **bright white lines** at the very top level of the grayscale. These signals **saturate** the receiver of the scanner.

49

### Ultrasound physics: reflection and transmission

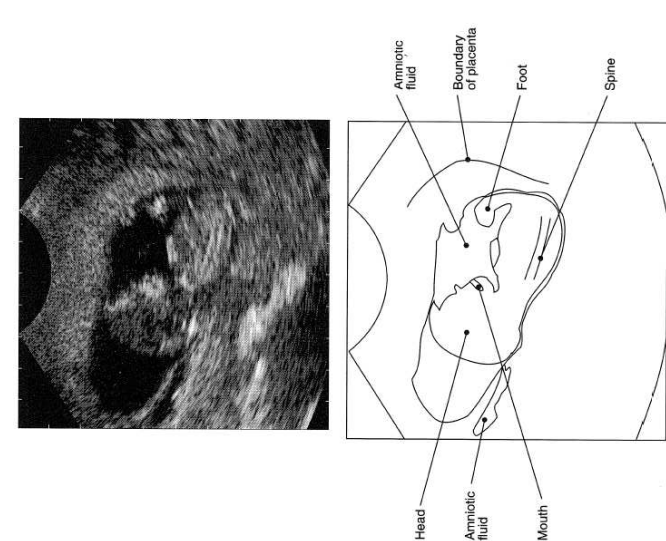


Fig. 2.4. Ultrasound images of 13th week fetus. The markers at the border of the image indicate one centimeter.

Source: Jensen p. 25

50

### Ultrasound physics: scattering

- In the previous figure, a B-mode scan of a fetus is shown. Even though there is a strong acoustic mismatch between the properties of skull and amniotic fluid, we do not see a strong skull outline because the **reflection does not return in the direction of the transducer**. The head of the fetus can be identified only from the **backscatter**.
- In the next figure, a close-up B-mode image of the liver is shown. In an MR image, we would see homogeneous liver tissue and two large blood vessels. In this ultrasound image, the homogeneous tissue appears **speckled**.
- Speckle is produced by **scattering** due to wave interaction with, for example, **blood cells, fibers and connective tissue**. These structures are smaller than the wavelength of the ultrasound.

51

### Ultrasound physics: scattering

- Because of this, the structures **cannot be resolved**. However, the **interference** (constructive and destructive) **patterns** that result give us insight into tissue composition. e.g. fat infiltration in liver tissue, tumors in the prostate.
- Scatterers range in size from blood cells ( $\approx 10\mu\text{m}$ ,  $0.03\lambda$  at 5 MHz) to organ boundaries ( $\approx 10\text{cm}$ ,  $300\lambda$  at 5 MHz).
- The boundary reflections we have already analyzed are the type of scatter that occurs when the **scatterer is much larger than the wavelength**. This is called scattering in the **geometrical region**. It is **independent of insonation frequency** and produces **strong scatter** signals

52

## Ultrasound physics: scattering

- **Diffractive scatter** occurs when the scatterer similar in extent to the wavelength. This is called scattering in the **stochastic region**. The interference pattern is highly **frequency dependent** and has **moderate power**.
- Scatter in the **Rayleigh region** occurs when a wave interacts with a scatterer that is **much smaller than the wavelength**. It is dependent on the **fourth power of the frequency** of the insonation. Rayleigh scatter is a **weak effect** and is produced, for example, at blood cells.

53

## Ultrasound physics: scatter

**Table 7.1** Types of scattering interaction classified according to the scale of the characteristic dimension  $a$  of the scattering structure relative to the wavelength  $\lambda$  of sound for frequencies typical of those used in medical imaging.

Scale of interaction	Frequency dependence	Scattering strength	Examples
$a \gg \lambda$ Geometrical region, ray theory for reflection and refraction	$f^0$	Strong	Diaphragm, large vessels, soft tissue/bone, cysts, eye orbit
$a \sim \lambda$ Stochastic region (diffractive)	Variable	Moderate	Predominates for most structures (even for examples in the other two categories)
$a \ll \lambda$ Rayleigh region	$f^4$	Weak	Blood

Source: Webb p. 324

54

## Ultrasound physics: scatter

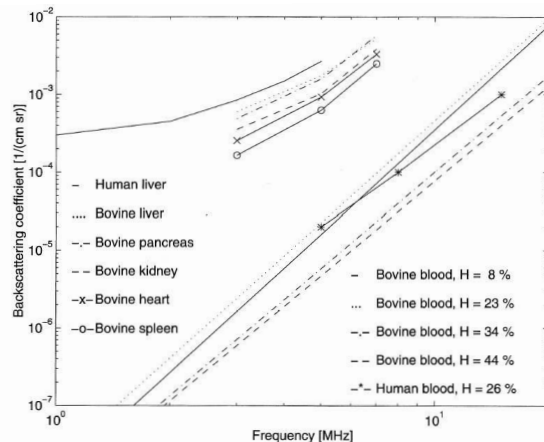


Fig. 2.6. Measured backscattering coefficients for human liver tissue, bovine myocardium, bovine kidney cortex, human spleen, and bovine and human blood as a function of frequency (data from Nicholas (1982), Fei and Shung (1985), Shung (1992), and Yuan and Shung (1988b)).

Source: Jensen p. 29

55

## Ultrasound physics: attenuation

Another important tissue property that leads to contrast in ultrasound images is **attenuation**.

- Attenuation is frequency dependent and **increases with insonation frequency**.
- We usually assume attenuation is **linearly proportional to distance traveled**. Linear attenuation coefficients have units of dB/(MHz cm).
- Attenuation is caused by:
  1. **Redirection** of energy due to **scattering**.
  2. **Absorption**. Conversion to thermal energy occurs due to **viscous loss, heat conduction and molecular energy exchange**.
- We wish to determine the attenuation of an applied ultrasound wave when investigating the prostate gland. We assume that an attenuation coefficient of 0.7dB/(MHz cm) applies. The prostate is at a depth of 10 cm. What is the attenuation?

56

## Ultrasound CT

- When diffraction effects can be ignored (a reasonable assumption in soft tissues only), **transmission ultrasound projections resemble x-ray CT projections**.
- US CT yields **two types of projections**:
  1. Amplitude changes between transmitted and received signals give **line integrals of the acoustic attenuation coefficients**.
  2. Since the speed of sound in tissues is **low compared to that of light**, the **time-of-flight** of ultrasound pulses is easy to calculate. **Time-of-flight values** at projection bins are proportional to **line integrals of the refractive index** of the tissues normal to that bin.
- Is conventional B-mode imaging tomographic?

---



---

- Why bother with US transmission CT?

---



---

57

## Ultrasound CT

- In order to perform US CT, a **layer of water or gel** must be employed to **match the transducers to the acoustic impedance of tissues**.
- Consider an applied US signal  $x(t)$  **transmitted through a single layer of tissue** that is received as  $y(t)$ . Then the FT of the received signal is the product of the following factors:
  1. The transmitter transfer function  $H_1(f)$  that relates the applied voltage to the pressure waveform.
  2. The attenuation factor  $e^{-\alpha_w(f)l_w^1}$  that accounts for the attenuation in the water layer near the transmitter.
  3. The phase change factor  $e^{-j\beta_w(f)l_w^1}$  that accounts for the propagation delay through the water layer near the transmitter.
  4. The transmittance at the near surface of the distribution  $\tau_1$ .
  5. The attenuation factor  $e^{-\alpha(f)l}$  that accounts for the attenuation in the tissue.

58

## Ultrasound CT

6. The phase change factor  $e^{-j\beta(f)l}$  that accounts for the propagation delay in the tissue.
7. The transmittance at the far surface of the distribution  $\tau_2$ .
8. The attenuation factor  $e^{-\alpha_w(f)l_w^2}$  that accounts for the attenuation in the water layer near the receiver.
9. The phase change factor  $e^{-j\beta_w(f)l_w^2}$  that accounts for the propagation delay through the water layer near the receiver.
10. The receiver transfer function  $H_2(f)$  that relates the incident pressure waveform to the voltage produced at the transducer.

Thus:

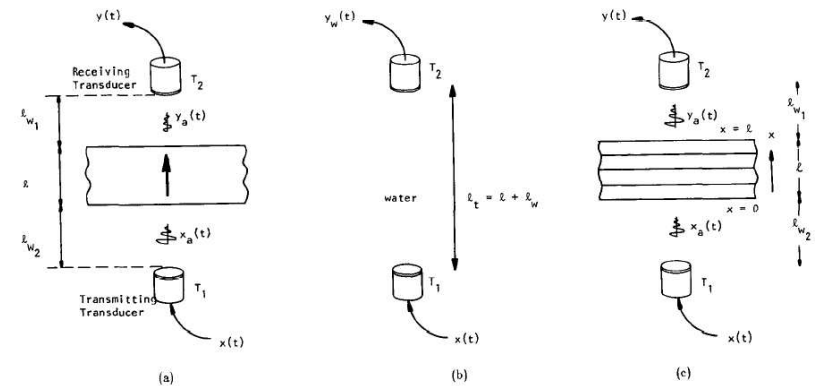
$$Y(f) = X(f)H_1(f)H_2(f)A_\tau e^{-(\alpha(f)+j\beta(f))l} e^{-(\alpha_w(f)+j\beta_w(f))l_w}$$

where

$$l_w = l_w^1 + l_w^2 \quad \text{and} \quad A_\tau = \tau_1 \tau_2$$

59

## Ultrasound CT



Source: Kak p. 149

An ultrasonic beam travelling between two transducers undergoes a phase shift in the water surrounding the imaged tissue layer and both a phase shift and attenuation in the tissue ( (a) and (b) ). In (c) the beam travels through water and a multilayered object.

60

## Ultrasound CT

- Because the attenuation in water is negligible, for a **multilayer object** we have:

$$Y(f) = X(f)H_1(f)H_2(f)A_\tau e^{-\int_0^l (\alpha(x,f) + j\beta(x,f)) dx} e^{-j\beta_w(f) l_w}$$

where  $A_\tau = \prod_{n=1}^N \tau_i$  is the product of the transmittances at the  $N$  layer interfaces.

- We can separate out the contribution to  $Y(f)$  of the water layers by defining:

$$Y_w(f) = X(f)H_1(f)H_2(f)e^{-(\alpha_w(f) + j\beta_w(f))(l + l_w)}$$

which corresponds to the **received signal in the absence of the tissue**.

- Then:

$$Y(f) = A_\tau Y_w(f) e^{-\int_0^l \alpha(x,f) dx} e^{-j2\pi f \int_0^l (1/c(x) - 1/c_w) dx}$$

where  $c(x)$  is the spatially dependent velocity of sound in the tissue and  $c_w$  is the velocity of sound in water.

61

## Ultrasound CT

- In order to separate the effects of attenuation and propagation delay, we now define:

$$y'_w(t) = \mathcal{F}_1^{-1} \left\{ A_\tau Y_w(f) e^{-\int_0^l \alpha(x,f) dx} \right\}$$

which can be interpreted as the “attenuated” water path signal. This is the **hypothetical signal that would be received if the ultrasonic pulse travelled through water, but experienced the same attenuation as occurs in the tissue**.

- The **true received signal** can then be expressed as a **delayed version of the hypothetical signal** (since we have modeled only attenuation effects of the tissue and not the effects of refractive index):

$$y(t) = y'_w(t - T_d)$$

where

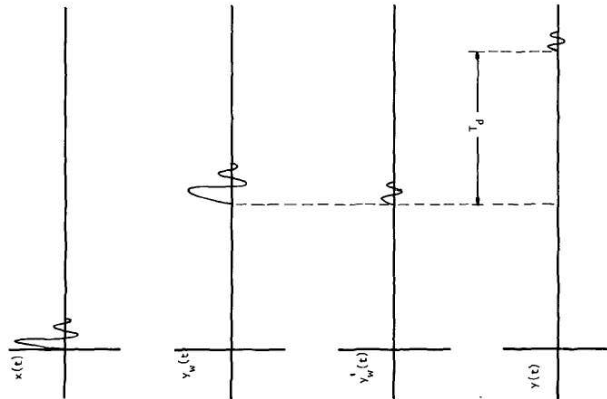
$$T_d = \frac{1}{c_w} \int_0^l (n(x) - 1) dx$$

where  $n(x)$  is the spatially dependent refractive index given by:

$$n(x) = \frac{c_w}{c(x)}$$

62

## Ultrasound CT



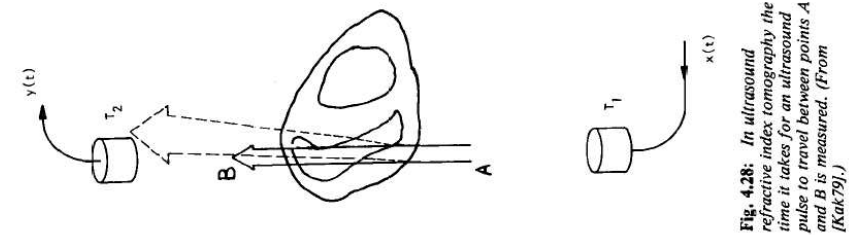
Source: Kak p. 152

The transmitted signal  $x(t)$  traveling only through water experiences a phase shift (time delay) and slight attenuation. Modeling the attenuation through tissue gives  $y'_w(t)$ . Including the propagation delay through the tissue (related to the refractive indices along the path) gives the received signal  $y(t)$ .

63

## Ultrasound refractive index CT

Consider the ray AB:



Source: Kak p. 153

The transmitted and received signals can be used to measure the right hand side of the line integral:

$$\int_A^B (1 - n(x, y)) ds = -c_w T_d$$

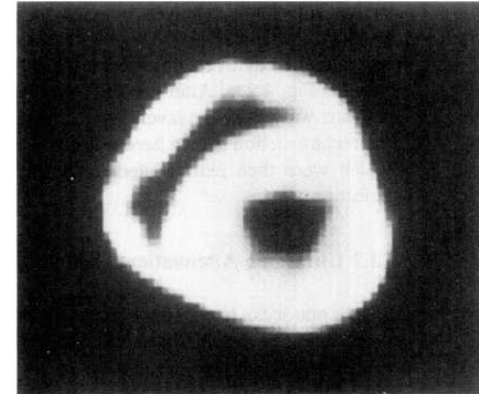
64

### Ultrasound refractive index CT

- By collecting enough line integrals to sample the  $n(x, y)$  adequately, the the **discrete Radon transform** of  $1 - n(x, y)$  can be collected.
- Conventional inverse RT methods yield the **distribution of refractive indices**.
- Usually, we wish to look at  $1 - n(x, y)$  since for the background (water),  $n(x, y) = 1$ . Water will consequently appear “black”.
- The propagation time of short ultrasound pulses is used to find the  $T_d$ . These delays of  $\approx 100 \mu s$  are easily measured using simple electronics.
- Since  $c(x, y)$  for tissues is usually greater than  $c_w$ , the right hand side of the line integral is usually positive, since  $T_d$  is usually negative.

65

### Ultrasound refractive index CT



Source: Kak p. 154

Refractive index tomographic reconstruction of slice through formalin-preserved dog heart. Could this technique be used for imaging cardiac structure in live humans? Explain.

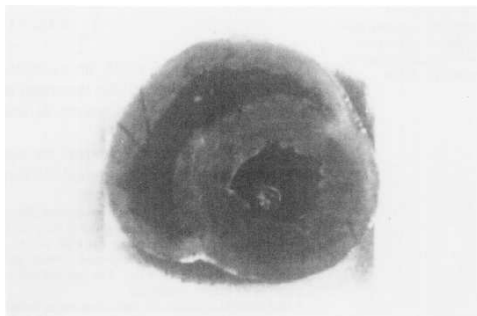
---



---

66

### Ultrasound refractive index CT



Source: Kak p. 154

Photograph of section through the dog heart imaged using ultrasound CT. Which organs in the human body might be effectively imaged using ultrasound CT?

---



---

67

### Ultrasound attenuation CT

- Let  $\alpha(x, y, f)$  represent the **acoustic attenuation coefficient** at point  $(x, y)$  for insonation at frequency  $f$ .
- Any attenuation distribution we reconstruct will be affected by the **frequency of insonation**.
- In soft tissues, the approximation:

$$\alpha(x, y, f) = \alpha_0(x, y)f$$

holds in the low MHz range.

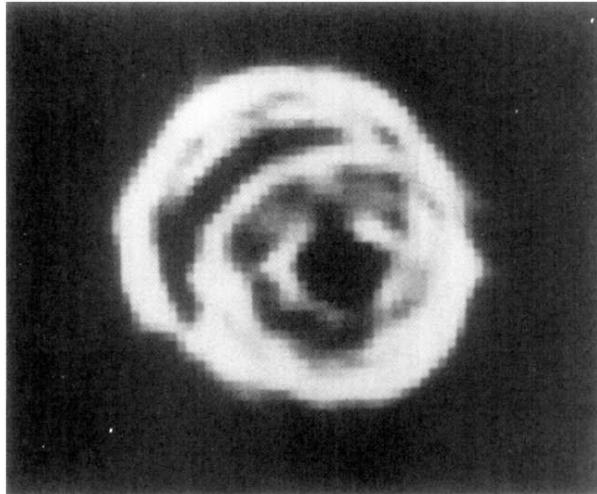
- The parameter  $\alpha_0(x, y)$  completely characterizes the soft tissue attenuation properties at  $(x, y)$ .
- The line integral of the attenuation is given by:

$$\int_A^B \alpha_0(x, y) ds$$

- Excitation at multiple frequencies (broadband pulsed CW) is required to measure the  $\alpha_0(x, y)$  distribution.

68

### Ultrasound attenuation CT

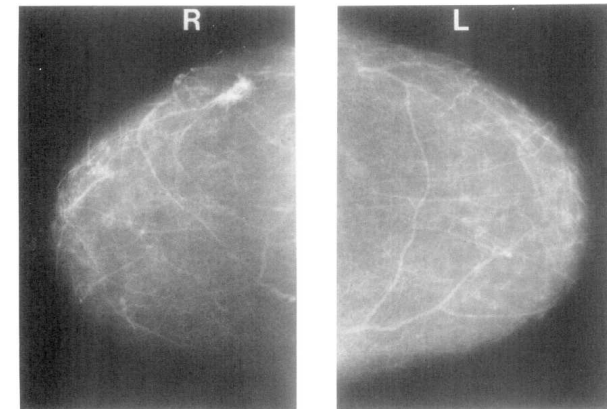


Source: Kak p. 158

Acoustic attenuation image of dog heart ( $\alpha_0[m, n]$ ).

69

### Ultrasound attenuation CT

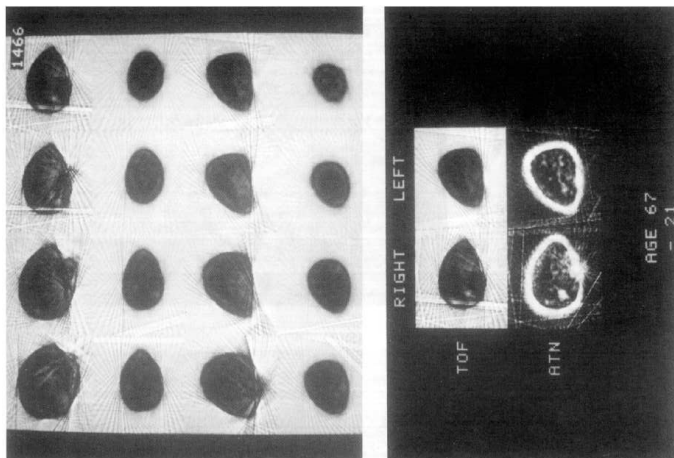


Source: Kak p. 159

These mammograms show a small cancerous tumor in the upper outer quadrant of the right breast.

70

### Ultrasound CT: clinical applications



Source: Kak p. 160

Both refractive index and attenuation images reveal the cancer using ultrasound transmission tomography. The upper image shows a set of parallel transverse slices.

71